DOI: 10.21062/mft.2025.020 http://www.journalmt.com

Modeling Method and Simulation of Crushing Process of Vertical Shaft Impact Crusher Based on Cumulative Damage Model

Canhui Wu (0009-0008-8314-1664), Limei Zhao (0000-0002-7718-8756)*, Song Li (0009-0009-3886-3358)
School of Mechanical Engineering, Guizhou University, Guiyang, China.
Corresponding author's E-mail: lmzhao@gzu.edu.cn

In a vertical impact crusher, material particles undergo multiple impact collisions and eventually break due to accumulated damage. In order to further study the crushing mechanism of the crusher, a cumulative damage model of material particles under repeated impact was established. Firstly, a crushing model is established based on the specific fracture energy, reflecting material particles' cumulative damage and crushing process. Then, the simulation model of the crushing system of the vertical shaft impact crusher is established. And by simulating the crushing process of limestone particles in a crusher, it reveals that the crushing of particles is essentially due to the crushing that occurs as a result of multiple cumulative impacts. Next, the simulation model is used to simulate and analyze the rotor's power and particle size distribution of crushed products of limestone, iron ore, and copper ore during crushing. The reliability of the simulation model is experimentally validated. Finally, the simulation analyzed the influence of the diameter and speed of the crusher rotor, as well as the mixed feeding of various materials, on the rotor power and material crushing effect. The results show that the particle size distribution curves of three types of crushed products, including limestone, have a high degree of agreement between simulation and experiment. Furthermore, the simulation values of rotor power and specific power consumption fit well with the experimental values, verifying the reliability of the simulation model. As the rotor diameter and rotor speed increase, the rotor power and sand production rate gradually increase. And the increase in rotor power is much greater than the increase in sand production rate. When the feed is a mixture of multiple materials, the rotor power increases approximately linearly with the increase of the proportion of high hardness materials in the feed, while the yield of fine particles in the crushed product decreases with the increase of the proportion of high hardness materials in the feed.

Keywords: Vertical shaft impact crusher, Cumulative damage, Power, Material crushing rate, Particle size distribution

1 Introduction

In recent years, the demand for sand is increasing with the development of infrastructure construction in countries worldwide [1-3]. However, since the reserves of natural sand are limited, using artificial sand instead of natural one has become an inevi Tab. trend [4-6]. Vertical shaft impact crusher has become a widely used crushing equipment in the sand industry due to its advantages of small size and good granularity of discharged material [7-11]. Studying the crushing mechanism of a vertical shaft impact crusher is significant for researching and developing an energy-efficient new type of crusher and optimizing crusher operating parameters [10]. However, due to the complexity of the mechanical structure and crushing environment, it is difficult to explore the crushing mechanism of the vertical shaft impact crusher using the experimental method [12]. In recent years, with the development of computer technology, simulation technology has been used to simulate the particle crushing process and provide new methods and ideas for studying the crusher crushing mechanism.

Segura-Salazar et al. successfully established the mathematical model of a vertical shaft impact crusher using the White crusher model. Moreover, the authors simulated the flow process of the material after it entered the crusher and investigated the effect of the rotor rotational speed on the rotor power. The authors concluded that the rotor power increases with the rotor rotational speed[13]. Sinnott and Cleary simulated the vertical shaft impact crusher's crushing process by observing the material particles' movement law. They found that the particles are crushed when subjected to the impact energy exceeding their threshold energy. Based on this, the authors established a mathematical model of material crushing, providing the theoretical basis for studying the crushing mechanism of the crusher using the discrete element method[14]. Djordjevic et al. used large material particles as the simulation object and several small particle clusters connected by bonding bonds to replace the large particles and represent the crushing effect of the material. The authors concluded that the crushing of materials in vertical axis impact crushers is mainly a form of impact

crushing in which materials collide with the crusher and materials collide with each other[9]. In addition, Fang et al. used discrete element software to simulate the motion characteristics of particles in the crusher, and the reliability of the discrete element simulation model is verified experimentally[15]. Luo et al. used simulation technology to study the structural and working parameters of a vertical impact crusher, and analyzed the influence of rotor diameter and speed on the power and crushing effect of the crusher rotor [16,17].

Although the application of discrete element simulation technology in the research of vertical shaft impact crushers has achieved significant strides, most simulation models only consider the one-time crushing form caused by collisions between material particles and anvil or material particles. But in the vertical impact crusher, the material particles are subjected to multiple impacts and collisions from the crusher structure and other material particles during the crushing process, and are crushed due to the accumulated damage caused by multiple impacts and collisions. Hence, the cumulative damage effect to the material particles is particularly important. Most existing studies neglect the cumulative damage effect of material particles during crushing. Furthermore, most feed particles are single spherical particles; this differs from real crushing and changes the contact state between material particles, crusher structure, and material particles. Consequently, the calculation of the impact force is affected, resulting in a significant difference between the simulation and the crushing experimental results. The simulation results of material crushing have a large error compared with those of crushing experiments.

Therefore, this article establishes a mathematical model for the cumulative damage of material particles under repeated impact. On this basis, a simulation model of the crushing system was established, including a polyhedral particle material model and a vertical axis impact crusher model. Then, a simulation model was used to analyze the particle size distribution and rotor power of three different materials with different characteristics, including limestone, and the reliability of the simulation model was verified through experiments. Finally, the constructed simulation model was used to analyze the effects of rotor diameter, rotor speed, and mixed feeding of various materials on the rotor power, crushing rate, and particle size distribution of the vertical shaft impact crusher, providing theoretical guidance for achieving efficient and energy-saving artificial sand crushing processing.

2 Mathematical model of material crushing based on the cumulative damage

The material crushed by the vertical impact crusher is mostly in the shape of a convex surface. In the crushing chamber, the contact of material particles occurs between various edges, surfaces, and points, and the crushing process of particles is extremely energy consuming. The normal force contact model allows for significant energy dissipation, while the hysteresis linear spring model can calculate the plastic energy dissipation during particle contact without adding additional simulation time [18]. Based on this, Consequently, the contact force model is computed in this paper utilizing the linear spring coulomb limit model for the force tangential component and the hysteretic linear spring model for the force normal component. The calculation of the normal contact force of material particles at the current moment during the crushing process is shown in equation (1).

$$F_t^n = \begin{cases} \min\left(K_{nl}s_n^t, F_n^{t-\Delta t} + K_{nu}\Delta s_n\right) & if\ \Delta s_n \geq 0 \\ \max\left(F_n^{t-\Delta t} + K_{nu}\Delta s_n, \lambda K_{nl}s_n^t\right) & if\ \Delta s_n < 0 \end{cases} \quad (1)$$

$$\Delta s_n = s_n^t - s_n^{t-\Delta t}$$

Where:

F_t^n and $F_n^{t-\Delta t}$ …The normal contact forces at the current time and the previous time step, respectively [N],

Δt…The step size [s],

Δs_n…The overlap amount when particles come into contact (its value is positive when particles are close to other particles or the crusher wall; when particles move away from them, their value becomes negative),

K_{nu} and K_{nl}…The stiffness under impact and impact unloading, respectively [N/m],

f…The a dimensionless constant.

In addition, the tangential contact force experienced by particles can be calculated using the linear spring Coulomb limit model.

$$F_{\tau,e}^t = F_\tau^{t-\Delta t} - K_\tau \Delta s_\tau \quad (2)$$

Where:

$F_\tau^{t-\Delta t}$ …The tangential force [N],

ΔS_τ…The relative tangential displacement in the time step [mm],

K_τ…The tangential stiffness [N/m], calculated as:

$$K_\tau = r_K K_{nl} \quad (3)$$

Where:

r_k…The tangential stiffness ratio.

Among them, there is a limit requirement for the tangential force exerted on particles, spe-cifically that the tangential force cannot exceed the Coulomb limit. Therefore, the complete expression of tangential force is:

$$F_\tau^t = \min\left(\left|F_{\tau,e}^t\right|, \mu F_n^t\right)\frac{F_{\tau,e}^t}{\left|F_{\tau,e}^t\right|} \quad (4)$$

Where:

F_τ^t …The contact normal force at time t,

u…Friction coefficient, defined as:

$$u = \begin{cases} u_s \text{ if no sliding takes place at the contact} \\ u_d \text{ if sliding does take place at the contact} \end{cases} \quad (5)$$

Where:

u_s…The static friction coefficient of particles,

u_d…The coefficient of dynamic friction of particles.

When the vertical shaft impact crusher operates, the material particles fall into the distributing cone of the high-speed rotor under the effect of gravity. The distributing cone disperses the material evenly to the guide plate. The material particles on the guide plate are accelerated to the outer edge of the rotor due to the centrifugal force and the squeezing force between the mate-rials. They are thrown out from the outlet of the guide plate at the end of the guide plate. The material particles undergo multiple impacts and collisions with the anvil installed in the cham-ber and other material particles in the crushing chamber during their movement, resulting in fragmentation[19]. It can be seen that the fundamental cause of material particle breakage is the accumulated damage caused by multiple impacts and collisions during its movement. There-fore, the crushing situation of material particles can be predicted based on the accumulated impact energy received by the material particles when they collide with the crusher structure or material particles inside the crusher. According to Tavares' research, each material particle has a specific fracture energy, which is only related to the size and shape characteristics of the particle itself[20-22].When the impact energy of a material particle exceeds its fracture energy, the parti-cle will break. The fragmentation probability is equal to the fracture energy distribution and is based on the upper truncated normal distribution function of the specific fracture energy [23], as shown in Eq. (6).

$$P_0(E) = \frac{1}{2}\left[1 + erf\left(\frac{lnE^* - lnE_{50}}{\sqrt{2\sigma_E^2}}\right)\right] \quad (6)$$

$$E^* = \frac{E_{max} * E}{E_{max} - E} \quad (7)$$

Where:

E^*…The relative specific fracture energy,

E…The specific fracture energy,

E_{50}…The median fracture energy,

σ_E…The variance of the distribution of fracture energies,

E_{max}…The upper cut-off value of the distribution.

Median fracture energy E50 is a power function based on particle size. The functional relationship is shown in Eq. (8).

$$E_{50} = E_\infty\left[1 + \left(\frac{d_0}{L}\right)^\varphi\right] \quad (8)$$

Where:

E_∞, d_0, and φ…The model parameters fitted to the experimental data,

L…The diameter of a representative particle in the particle population [mm].

The crushing of particles in a vertical shaft impact crusher is mainly cumulative impact crushing. Therefore, it is crucial to consider the cumulative damage effect of materials. In other words, when the impact energy of particles is lower than their initial fracture energy, the internal structure of the particles will be damaged, and the particles will be internally cracked. However, such impact energy does not cause the particles to be directly crushed. At this time, the fracture energy of the particles decreases, and the particles are crushed when their impact energy is gradually reduced to 0. In continuous damage to the particles, the reduction of their fracture energy can be expressed by the mathematical expressions of Eqs. (9) and (10):

$$E_n = E_{n-1}(1 - D_n^*) \quad (9)$$

$$D_n^* = \left(\frac{2\gamma}{\left(2\gamma - 5D_n^* + 5\right)}\frac{E_{k,n}}{E_{n-1}}\right)^{\frac{2\gamma}{5}} \quad (10)$$

Where:

E_n…New fracture energy of the particles formed after the nth impact [J/kg],

$E_{n\text{-}1}$…The fracture energy of the particles before the nth impact [J/kg],

D_n^*…The amount of damage to the particles resulting from the nth impact,

$E_{k,n}$…The the energy of the nth impact [J/kg],

γ…The damage constant.

Once the material particles are crushed, the produced sub-particles will continue to repeat the above process until their impact energy is zero. The particle size distribution law of sub-particles is determined by defining the value of t10 [22], as shown in Eq. (11):

$$t_{10} = A\left[1 - exp(-b' \cdot \frac{E_k}{E_{50b}})\right] \quad (11)$$

Where:

t_{10}…The percentage of the mass of the crushed product under the sieve in which the particle size is smaller than the original particle size $L/10$,

E_k…The impact energy,

E_{50}…The media fracture energy of the particles that did break in the impact,

σ_E…The variance of the distribution of fracture energies,

A…The maximum value reached by t10,

b'…The function coefficient.

The complete particle size distribution of the crushed product is defined quadratically by the Gaudin-Schuman model, which is a predicted particle size distribution law based on t10 and calculated as follows:

$$\gamma = 10t_{10}\left(\frac{x}{L}\right) \quad (12)$$

Where:

γ…The cumulative percentage of crushed particles,

x…The screen size during screening [mm],

L…The particle size before crushing [mm].

3 Simulation modelling

3.1 Establishing the 3D models

The research object of this article is the PL8500 vertical impact crusher, as shown in Fig. 1. The power of the vertical impact crusher is output by a motor and transmitted to the main shaft assembly through a belt drive, which drives the rotor to rotate continuously to accelerate the material.

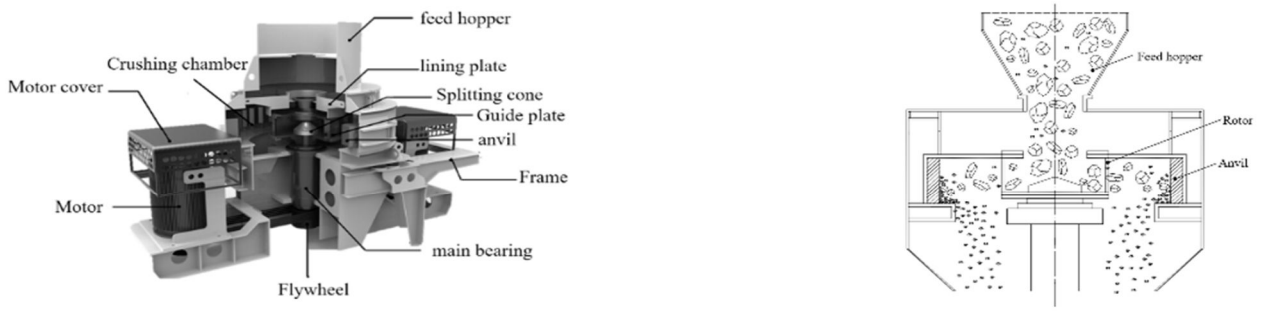

(a) Vertical impact crusher structure (b) Principle diagram of crusher

Fig. 1 *Structure and principle of vertical impact crusher*

From Fig. 1, it can be seen that during the operation of the crusher, the crusher system is mainly composed of a rotor body and a crushing chamber. The rotor mainly provides power for the materials entering the crusher, while the crushing chamber mainly serves as the place for material crushing. The excess structures and secondary features in the rotor body and crushing chamber will greatly reduce computational efficiency, and these structures and features have little impact on the calculation results, so they can be simplified. This article simplifies the structures of the feeding cone, feeding head, anvil sharp corner, etc., while removing the struc-tures of the feeding hopper, motor, motor cover, main bearing, and frame. The simplified crusher model is shown in Fig. 2.

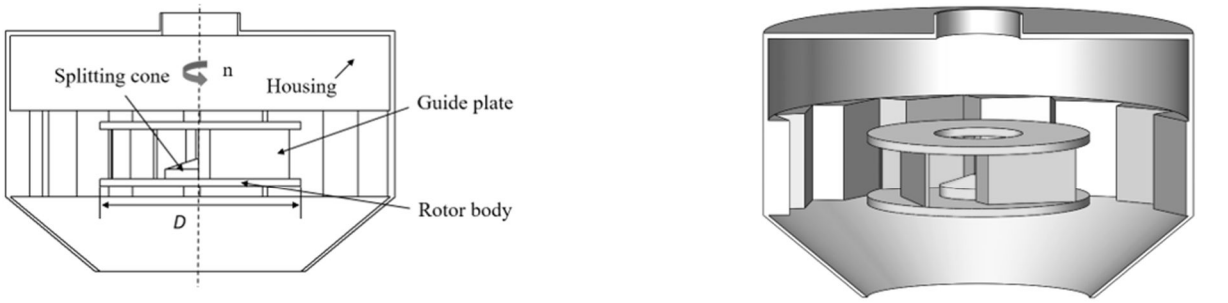

(a) Two dimensional model of crusher (b) Three dimensional model of crusher

Fig. 2 *Schematic diagram of analysis model for vertical impact crusher*

In the simulation modeling of crushers, most existing research uses EDEM and PFC to achieve it. However, this type of software not only has significant limitations in modeling parti-cle shapes but also has a slow calculation process, making it unsuiTab. for studying high-capacity crushers such as vertical impact crushers. Rocky DEM not only allows for quick creation of particle shape models within the software, but also supports the import of CAD parti-cle models in various intermediate formats such as STL. In addition, it adopts shared multi-core and multi-threaded parallel computing technology, which can fully utilize the computing performance of the graphics workstation without network transmission limitations, greatly improving the computing speed. The software also integrates multiple fragmentation models to predict the degree of particle fragmentation, achieving industry-leading computing power and accuracy [25-27]. Therefore, this article uses Rocky DEM (Rocky DEM 2022 R1.2) soft-ware to simulate and study the vertical impact crusher. The simplified three-dimensional model of the vertical impact crusher was imported into Rocky DEM software to obtain the simula-tion model of the crusher as shown in Fig. 3.

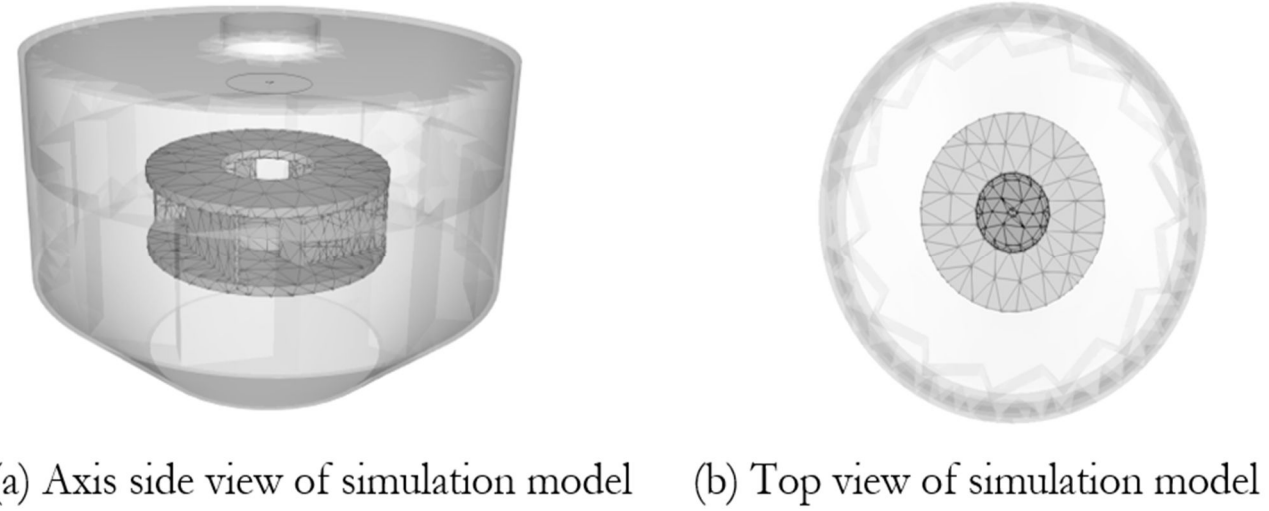

Fig. 3 *Physical Model of the Crusher*

3.2 Simulation parameter settings

When the crusher operates, the rotor rotates about the central axis of the rotor at a certain speed. Hence, the steering and rotation speed of the rotor needs to be set to 1200 r/min counterclockwise in the software. In addition to setting the correct movement of the VSI crusher, the physical parameters of the main structure of the rotor must also be set to facilitate the rotor's dynamic analysis, including the rotor's volume, mass, and moment of inertia. The volume and the position of the rotor's center of gravity were determined using SolidWorks. The moment of inertia of the rotor was calculated from the geometry and physical parameters of the rotor, as shown in Tab. 1.

Tab. 1 *Physical properties of the rotor*

Parameter		Value	Unit
Volume		4000	cm^3
Mass		287.67	kg
Moment of inertia	Px	14.37	$kg.m^2$
	Py	14.37	
	Pz	22.51	

3.3 Material and contact parameters

Three materials with different crushing characteristics, namely limestone, iron ore, and copper ore, are selected for simulation tests in this paper. The particle sizes of the materials are all in the range of 20-60 mm.

In addition, it is also necessary to set the contact model parameters of the material and the corresponding material property parameters. The contact model parameters of some materials and the material property parameters of the particles are given in Tabs. 2 and 3, respectively, where limestone-limestone indicates the contact parameters between limestone and limestone. Limestone-crusher indicates the contact parameters between the limestone and the crusher [12].

Tab. 2 *Contact model parameters*

Physical parameter	Limestone - Limestone	Limestone-Crusher
Static friction	0.5	0.6
Kinetic friction	0.01	0.01
Coefficient of restitution	0.1	0.2

Tab. 3 *Material property parameters*

Physical parameter	Limestone	Crusher
Poisson's ratio	0.218	0.28
Densities (kg/m3)	2700	7800
Young's modulus (Pa)	1.54×10^{10}	2.4×10^{11}

The particle shape of the material crushed by the vertical impact crusher in actual operation is not a single shape. Due to the need to reduce computation time, existing literature often uses single shaped material particles for simulation. However, only a single shape of the material particles is used for simulation experiments. However, when only using single shaped material particles for simulation experiments, it will cause gaps between particles that do not match the actual situation, affecting the contact state and interaction force between particles, and thus affecting the motion trajectory and crushing situation of materials in the crushing chamber, seriously affecting the accuracy of simulation results [28,29]. Therefore, the simulation model of four kinds of limestone particles shown in Fig. 4 was established according to the shape of the limestone particles in the actual crushing operation and the mass percentage of each shape. It was determined that the mass percentage of each particle under the same particle size was 30 %, 25 %, 25 %, and 20 %. Its surface characteristics covered the approximate spherical particles to the sharp-edged polyhedral particles.

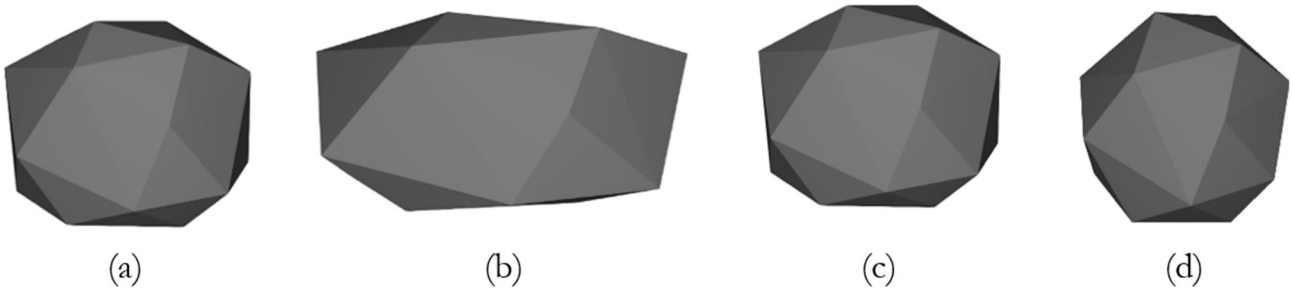

Fig. 4 *Particle model of four types of granular materials*

3.4 Crushing model parameters

Fitting the crushing model parameters of materials from single particle impact crushing experiments using ultrafast load sensors[30]. As shown in Tab. 4. The minimum size of the material particles formed after crushing is set to be 2 mm to reduce the amount of arithmetic without affecting the conclusions of the simulation and analysis, i.e., the minimum feed particle size (20 mm) in the simulation of the 1/10[31].

Tab. 4 *Material particle crushing parameters*

Crushing parameter	Limestone	Iron Ore	Copper ore
σ^2	0.09	0.2116	0.16
E_{max}/E_{50}	4	4	4
E_∞ (J/kg)	150	44.9	60
d_0 (mm)	0.79	4.3	400
φ	1.3	1.28	0.45
γ	5	3	5
A	0.634	0.604	0.677
b	0.033	0.051	0.029

4 Results and discussion

4.1 Experimental validation

After the simulation is completed, a moment in the limestone simulation process is selected as shown in Fig. 5. From Fig. 5 (a), it can be seen that during the crushing process of the vertical axis impact crusher, the material is distributed to each guide plate through the dividing cone. After being accelerated by the guide plate, a material flow is formed, and at the turning point of the material flow trajectory, it collides with the guide plate and anvil in sequence. From Fig. 5(b), it can be seen that the collision between the material and the guide plate occurs at the turning point of the guide plate, and is also subjected to impact, collision, and compression from particles of other materials. Some of the material that has reached the crushing limit due to damage accumulation will be crushed, while some of the material that has not reached crushing conditions will continue to be thrown along the guide plate. As can be seen from Fig. 5(c), most of the material thrown along the guide plate is crushed by impact collision with the anvil or other materials. After crushing, the sub-particles that still have large impact energy will continue to be crushed by impact collision with the material thrown from the guide plate. The guide plate is thrown out of the material and crushed. Crushed material drops due to the gravitational force and escapes through the discharge port, as shown in Fig. 5(d).

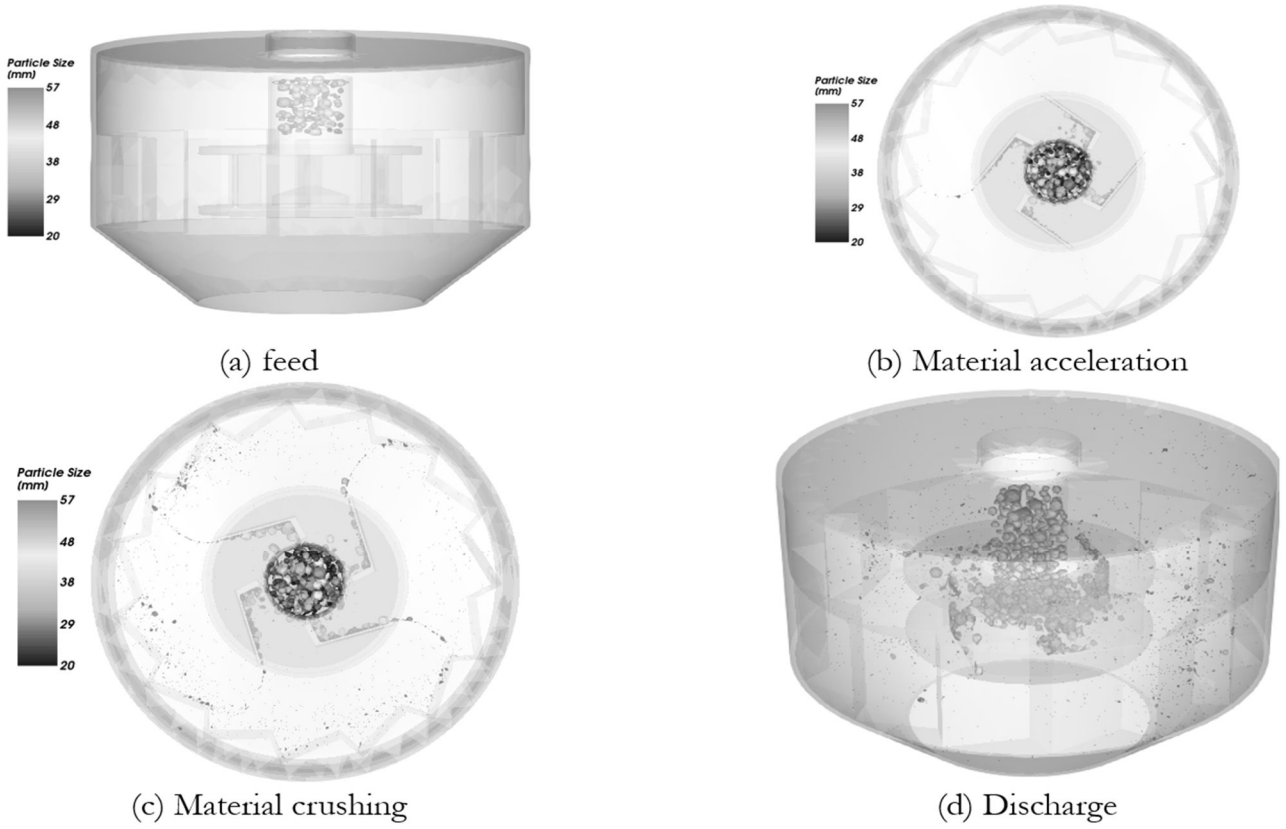

Fig. 5 *The simulation process (particles are colored according to their size)*

Fig. 6 *Working site of a VSI crusher*

In order to verify the reliability of the simulation model, the PL8500 vertical shaft impact crusher is used in this paper for the experimental verification of the simulation model under the same operating conditions as the simulation. The experimental site is shown in Fig. 6. The bulk materials used in the experiments were taken from limestone particles extracted from the sand and gravel quarry of Hongjiadu Power Station, and iron ore and copper ore particles supplied by the co-operating companies. In order to adapt to the experimental requirements, the feed size was determined to be 20-60 mm, which was used as the experimental material. There are 5 stone sieves, all of them are iron plate round hole sieves with holes of

5 mm, 20 mm, 40 mm and 60 mm, which are used to sieve the materials. According to the operating parameters in the actual work of the crusher, the parameter ranges of rotor speed and feed rate are selected, and the rotor speed is set at 1200 rpm, and the feed rate are both 120 t/h for crushing test. The crushed product is sampled on a conveyor belt with a belt speed of 2 m/s, a sampling length of 2m and a sampling mass of approximately 34.6 kg. The crushed product was sieved and analysed using iron plate circular hole stone sieve and electronic bench scale to obtain the crushed product size distribution as shown in Fig. 7. Fig. 7(a) and 7(b) show the particle size distribution curves of the three materials under simulation and experimental conditions, respectively.

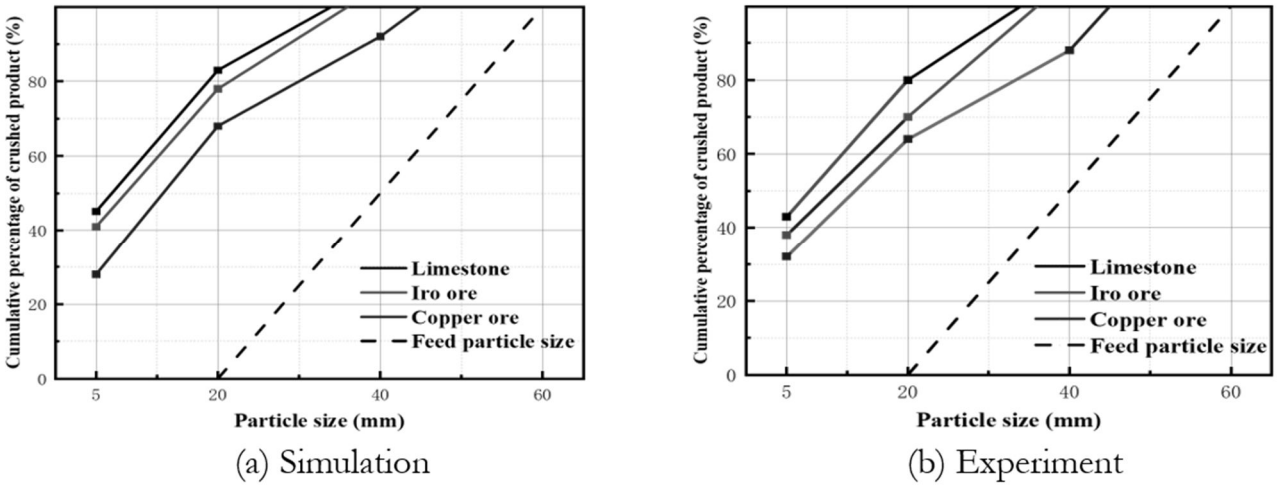

Fig. 7 *Particle size distribution curve of three materials*

As can be seen in Fig. 7, the shape of the particle size distribution curves of the three materials after crushing is similar, and the percentage of the crushed product under the sieve increases with particle size. However, the percentage of the crushed product passing through the screen for the limestone material at the same particle size is the largest, followed by iron ore and, fi-nally, copper ore, indicating that the lower the strength of the material, the easier it is for the material to be broken (under the same conditions). In addition, the slope of the curve is rela-tively large for particle sizes in the range of 5-20 mm. This indicates that the particle size distri-bution of the crushed products is mainly concentrated in the medium particle size, and the yield of coarser and finer sand and gravel is reduced. In order to more intuitively demonstrate the accuracy of the simulation system, the particle size distribution after crushing was statistical-ly analyzed, as shown in Tab. 5.

Tab. 5 *Particle size distribution of crushed products under simulation and experimentation*

Size	Simulation			Experiment			Relative error		
	Limestone	Iron Ore	Copper ore	Limestone	Iron Ore	Copper ore	Limestone	Iron Ore	Copper ore
-5mm (%)	45.1	41	28	43	38	32	5	7	14
-20mm (%)	83	78	68	80	70	64	3	10	20
-40mm (%)	100	100	92	100	100	88	0	0	4

As can be seen from Tab. 5, the maximum relative error in the cumulative mass percentage of the three materials under the crushing experiment and the simulation test is 20%. Therefore, the simulation model of the crushing system established in this article has high reliability.

In addition, the instantaneous rotor power change curve of three materials (such as limestone) during crushing is shown in Fig. 8. In Fig. 8, the power refers to the useful power, i.e., the instantaneous power consumed by the rotor calculated by multiplying the torque applied by the rotor to the material and the rotor speed. According to Fig. 8, the influence of materials with different crushing characteristics on the power consumption of the rotor can be well reflected through model simulation.

Limestone crushing simulation is taken as an example. The material starts to gradually enter the

inside of the rotor at approximately 0.2 s, and the instantaneous power of the rotor starts to fluctuate. At 0.2~0.3s, the amount of material entering the rotor gradually increases, resulting in a gradual increase in rotor power. After 0.3 s, the power curve of the rotor fluctuates around the horizontal line of 89.4 kW, indicating that the quantity of the material in the rotor reaches dynamic stability. The instantaneous power of the rotor reaches a relatively sTab. state. Among them, some materials will bounce back to the rotor after colliding with the anvil, thereby applying greater resistance torque to the rotor, resulting in peak instantaneous power of the rotor at certain time points.

Fig. 8 also compares the instantaneous power of the rotor when crushed in a VSI crusher for three materials. Due to the different crushing characteristics of the three materials, the instantaneous power of the rotor will remain sTab. at three different levels. The strength, density, and quality of limestone materials are relatively low, so they often break at lower energy, resulting in a smaller resistance torque applied to the rotor and a relatively lower instantaneous power of the rotor. However, due to the strength of the limestone being the lowest of the three observed materials, as the strength of the material increases, higher impact energy is required to crush these materials. Consequently, the resistance torque applied to the rotor increases, resulting in the instantaneous power of the rotor gradually increases.

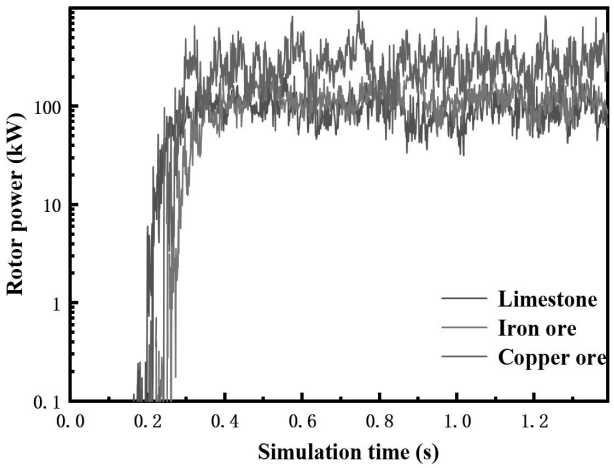

Fig. 8 *Instantaneous power of rotor under simulation conditions*

Tab. 6 *Comparison of simulated and experimental values*

	Material	Limestone	Iron Ore	Copper ore
Throughput (t/h)	Simulation	120	120	120
	Experiment	120	120	120
Power (kW)	Simulation	89.4	116.9	296
	Experiment	218	258	446
Specific power consumption (kWh/t)	Simulation	0.745	0.974	2.47
	Experiment	1.81	2.15	3.72
Power standard deviation	Simulation	47.4	126.9	137.6
	Experiment	32.3	86.42	126.7

This paper also compares the rotor power and specific power consumption when the simulation reaches the steady state with the experimentally calculated rotor power and specific power consumption to illustrate the reliability of the simulation model, as shown in Tab. 6. The results indicate that although the simulation and experimental results of rotor power and specific power consumption are not completely identical, the trend of change is the same. In this case, the specific energy consumed by the crusher during smooth operation of the crusher is 1.81, 2.15 and 3.72, while the specific power consumption of the rotor under the simulation is 0.745, 0.974 and 2.47, which is 41%, 45% and 33.7% of the specific energy consumed by the crusher, respectively. This is consistent with the findings of André, F. P and G. Unland [31,32]. The main reasons for this difference are as follows: Firstly, the vertical shaft impact crusher mainly provides kinetic energy for the rotor through the belt transmission of torque, increasing the energy dissipation in the transmission process. Secondly, the crushing parameters used in the simulation are estimated from the crushing experiments of single particles, causing the difference between the two.

4.2 Influence of rotor's diameter on material crushing

In order to facilitate the evaluation of the crushing efficiency of the vertical impact crusher and explore the influence of rotor structure parameters and working parameters on the crushing effect of the crusher. Based on the actual production needs of a certain enterprise in Guizhou, this article defines the sand production rate as the material yield passing through a 5mm sieve after crushing, which is used to characterize the crushing efficiency of the crusher. Under the conditions of rotor speed of 1200 r/min, feed particle size of 20-60 mm, and feed rate of 120t/h, three different materials were fed: limestone, iron ore, and copper ore. The influence of rotor

diameter variation in the range of 750mm~900mm on the rotor power and crushing rate of the vertical shaft impact crusher was analyzed, as shown in Fig. 9 and 10.

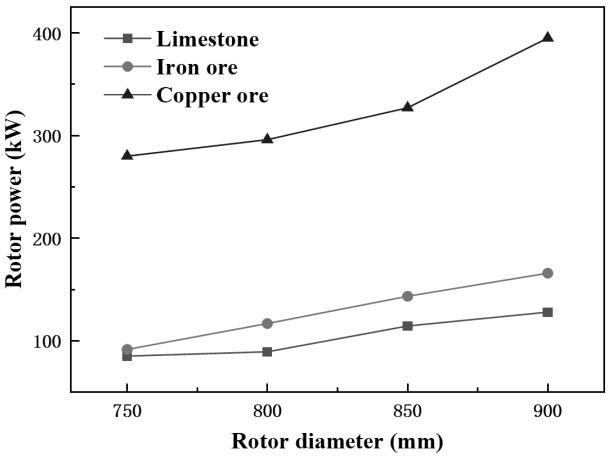

Fig. 9 *Effect of rotor diameter on rotor power*

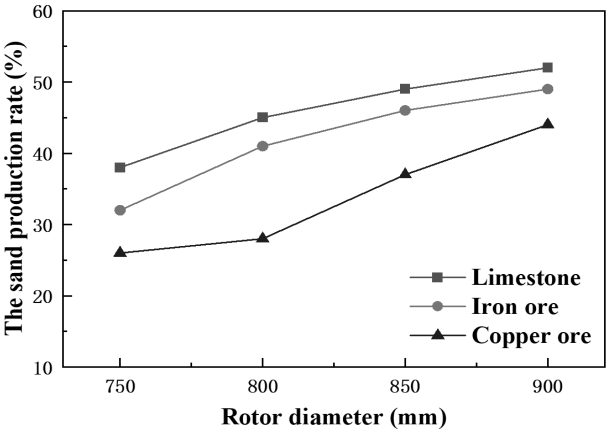

Fig. 10 *Effect of rotor diameter on crushing rate*

According to Fig. 9 and 10, the rotor power and sand production rate gradually increase with the rotor's diameter, in which the maximum value is reached when the rotor diameter is 900 mm. As the rotor's diameter increases from 750 mm to 900 mm, the rotor power under three different materials increases from 85.2 kW, 91.6 kW, and 279.9 kW to 128.2 kW, 166.8 kW, and 395.5 kW, with an increase of 50.5%, 82.1%, and 41.1%, respectively. The crushing rate increases from 38%, 32%, and 28% to 52%, 49%, and 44%, i.e., an increase of 36.8%, 53.1%, and 57.1%, respectively. The growth of rotor power is significantly greater than the growth of the crushing rate. It can be seen that increasing the rotor diameter can improve the crushing rate. However, it will make the rotor power increase significantly. Moreover, with an increase in the rotor's diameter, the design and manufacturing of the entire crusher equipment will also have a greater impact. Therefore, choosing a reasonable rotor diameter is important and consistent with the conclusions obtained from the literature [16,17].

4.3 Influence of rotor speed on material crushing

The rotor's diameter is 800 mm, the solids feed rate is 120 t/h, the feeding speed is 4.5m/s, the feed is limestone, iron ore, and copper ore, and the feed gradation is 20-60 mm. The remaining parameters are kept constant. The rotor speed is set to 1000 r/min, 1200 r/min, 1400 r/min, and 1800 r/min, respectively. The relationship between the rotor's power, the sand production rate, and the rotor speed is obtained, as shown in Fig. 11 and 12.

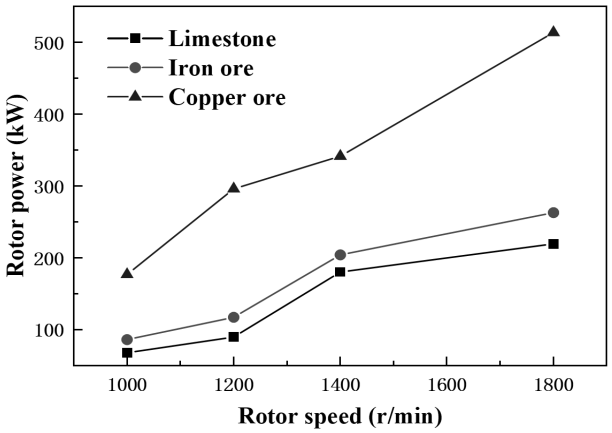

Fig. 11 *Effect of rotor speed on rotor power*

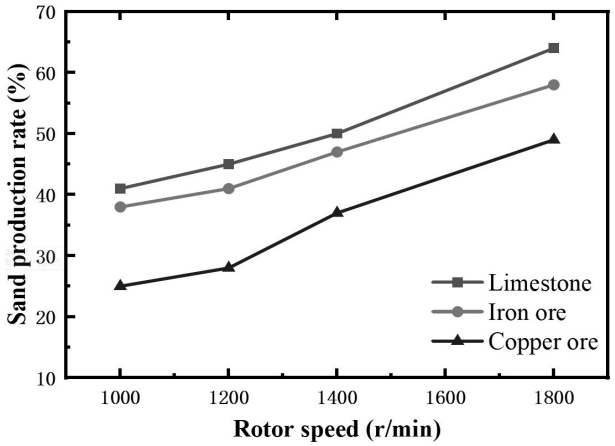

Fig. 12 *Effect of rotor speed on crushing rate*

Fig. 11 and 12 show that the rotor power and sand production rate gradually increase with speed. When the rotor speed increases from 1000 r/min to 1800 r/min, the rotor power under the three different materials increases from 67.6 kW, 85.8 kW and 176.5 kW to 324.1 kW, 363.9 kW, and 513.8 kW, i.e., the growth rate is 379.3%, 324.1%, and 191.1%. The sand production rate increases from 42%, 38%, and 28% to 64%, 58%, and 49%, i.e., the growth rate is 52.9%, 52.6%, and 75%. The growth rate of the rotor's power is larger than the increase of the sand production rate.

4.4 The effect of mixed feed on material crushing

A vertical shaft impact crusher is widely used for crushing various rocks and ores. Therefore, the

influence of mixed feeding of multiple materials on the crushing effect of the vertical shaft impact crusher was simulated. The rotor's diameter is 800 mm, its speed is 1200 r/min, and the solids feed rate is 120 t/h. The influence of mixed feed on the rotor power and particle size distribution of the VSI crusher is simulated and analyzed when the feed contains different proportions of limestone and copper ore.

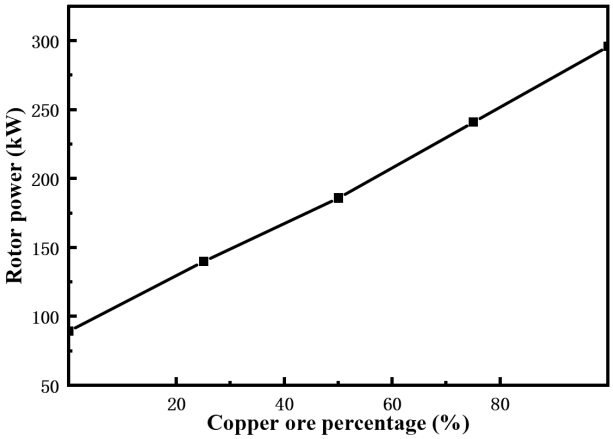

Fig. 13 *Effect of percentage of copper ore in the mixture on rotor power*

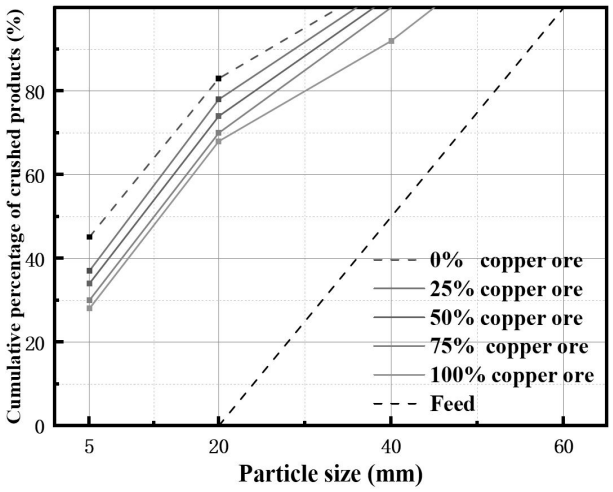

Fig. 14 *Effect of percentage of copper ore in the mixture on the particle size distribution*

The effect of mixtures containing different percentages of copper ore and limestone in the feed on the rotor power is shown in Fig. 13. As expected, the rotor power increases approxi-mately linearly as the proportion of high-hardness material (copper ore) in the feed increases from 0% to 100%, i.e., the rotor power increases with the proportion of high hardness material in the feed, which agrees with the conclusions in Section 4.1. The effect of increasing copper ore content on the particle size distribution of the crushed product when the mixture is fed is shown in Fig 14. It can be seen that the proportion of fine particles in the crushed product gradually decreases with an increase in the copper ore content in the mixture. Although not many investigations can be found regarding the crushing effect of the VSI crusher when the mixture is fed, this conclusion is consistent with the study's results on the effect of the mixture on the crushing effect of the cone crusher and ball mill [30,34,35]. In other words, when in-creasing the proportion of high-hardness materials in the feed, the yield of fine materials in the crushed product will gradually decrease.

5 Conclusions

In this paper, a simulation model of a vertical shaft impact crusher was established based on the cumulative damage model of material particles under repeated impact. By simulating the crushing process of limestone particles in the crusher, it is found that the crushing of materials in the crusher is mainly subjected to the cumulative impacts from the dividing cone, guide plate and anvil, and finally reaches the limit of particles' damage so that crushing occurs. In addition, the simulation and experimental values of particle size distribution and crusher rotor power of three kinds of crushed materials, such as limestone, were compared. The results show that the particle size distribution curves under simulation and experiment are in good agreement, and the trends of rotor power and specific power consumption are consistent.

The established simulation model was used to explore the influence of the rotor's structure and the operating parameters of the crusher on its performance. The results show that the constructed crushing simulation model is consistent with the related research, i. e. different materials show that the crushing rate increases with the rotor's diameter and rotational speed. Moreover, the rotor's power increases dramatically with the rotor diameter and rotational speed. And the growth rate of rotor power is greater than the growth rate of material crushing.

Simulation results on the effect of mixed feed on material crushing show that the rotor power increases approximately linearly with an increase in the proportion of high-hardness materials in the mixed feed under the same conditions. In contrast, the content of fine-grained materials in the crushed product gradually decreases.

Acknowledgement

This work was financially supported by The National Natural Science Foundation of China (No.52065007).

References

[1] BENGTSSON, M. Modelling energy and size distribution in cone crushers. *Minerals Engineering* 2019. DOI: 10.1016/j.mineng.2019.105869.

[2] JIANG, C.; GOU, D.; LI, C.; WU, G.; AN, X.; WANG, J.; GUO, P. Crushing characteristics and performance evaluation of iron ore in a cone crusher: A numerical study. *Minerals Engineering* 2023. DOI: 10.1016/j.mineng.2023.108429.

[3] KE SUN, LIMEI ZHAO, QITAO LONG. Optimization of Process Parameters for a Vertical Shaft Impact Crusher through the CFD-DEM Method. *Manufacturing Technology*, 2024.

[4] CANHUI WU, LIMEI ZHAO, CHENG ZHANG. Design and Simulation of Secondary Acceleration Type Rotor for Vertical Shaft Impact Crusher. *Manufacturing Technology*, 2024.

[5] ARTYUKHOV, ARTEM JAN KRMELA, VLADIMIRA KRMELOVA. Manufacturing of Vortex Granulators: Simulation of the Vortex Fluidized Bed Functioning under the Disperse Phase Interaction in the Constrained Motion. *Manufacturing Technology* 2020, 20(5): 547-53.

[6] LIU, R.; SHI, B.; LI, G.; YU, H. Influence of Operating Conditions and Crushing Chamber on Energy Consumption of Cone Crusher. *Energies* 2018. DOI: 10.3390/en11051102.

[7] AL-KHASAWNEH, Y. Novel design modeling for vertical shaft impactors. *Powder Technology* 2023. DOI: 10.1016/j.powtec.2023.119205.

[8] CLEARY, P. W.; DELANEY, G. W.; SINNOTT, M. D.; CUMMINS, S. J.; MORRISON, R. D. Advanced comminution modelling: part 1 – crushers. *Applied Mathematical Modelling* 2020. DOI: 10.1016/j.apm.2020.06.049.

[9] DJORDJEVIC, N.; SHI, F. N.; MORRISON, R. D. Applying discrete element modelling to vertical and horizontal shaft impact crushers. *Minerals Engineering* 2003. DOI: 10.1016/j.mineng.2003.08.007.

[10] NUMBI, B. P.; Xia, X. Optimal energy control of a crushing process based on vertical shaft impactor. *Applied Energy* 2014. DOI: 10.1016/j.apenergy.2014.12.017.

[11] WANG, C.; WANG, H.; OESER, M.; MOHD HASAN, M. R. Investigation on the morphological and mineralogical properties of coarse aggregates under VSI crushing operation. *International Journal of Pavement Engineering* 2020. DOI: 10.1080/10298436.2020.1714043.

[12] WU, C.; ZHAO, L.; CAO, Z. Collision Energy Analysis within the Vertical Shaft Impact Crusher Based on the Computational Fluid Dynamics-Discrete Element Method. *ACS Omega* 2024. DOI: 10.1021/acsomega.3c08017.

[13] SEGURA-SALAZAR, J.; BARRIOS, G. P.; RODRIGUEZ, V.; TAVARES, L. M. Mathematical modeling of a vertical shaft impact crusher using the Whiten model. *Minerals Engineering* 2017, 111, 222-228.

[14] CLEARY, P. W.; SINNOTT, M. D. Simulation of particle flows and breakage in crushers using DEM: Part 1 – Compression crushers. *Minerals Engineering* 2015, 74, 178-197.

[15] B, H. F. A.; B, J. Y. A.; C, Y. S.; D, W. H.; D, J. C. Simulation and experimental study on the stone powder separator of a vertical shaft impact crusher - ScienceDirect. *Advanced Powder Technology* 2020, 31 (3), 1013-1022.

[16] DA CUNHA, E. R.; DE CARVALHO, R. M.; TAVARES, L. M. Simulation of solids flow and energy transfer in a vertical shaft impact crusher using DEM. *Minerals Engineering* 2013, s 43–44, 85–90.

[17] LUO, M.; YANG, J. H.; FANG, H. Y. An Investigation on Sand Production of Vertical Shaft Impact Crusher Using EDEM. *Advanced Materials Research* 2014, 1004-1005, 1226-1230.

[18] WALTON, O. R.; BRAUN, R. L. Viscosity, granular-temperature, and stress calculations for shearing assemblies of inelastic, frictional disks. *Journal of Rheology* 1998, 30 (5), 949-980.

[19] WU, C.; ZHAO, L.; CAO, Z. The Crushing Distribution Morphology of a Single Particle Subjected to Rotary Impact. *ACS Omega* 2024. DOI: 10.1021/acsomega.4c00997.

[20] KING, R. P. Modeling of particle fracture by repeated impacts using continuum damage mechanics. *Powder Technology* 2002.

[21] LØLAND, K. E. Continuous damage model for load-response estimation of concrete. *Cement & Concrete Research* 1980, 10 (3), 395-402.

[22] TAVARES, L. M. Analysis of particle fracture by repeated stressing as damage accumulation. *Powder Technology* 2009, 190 (3), 327-339.

[23] KING, R. P.; Bourgeois, F. Measurement of fracture energy during single-particle fracture. *Minerals Engineering* 1993, 6 (4).

[24] IMAI, H.; IRI, M.; MUROTA, K. Voronoi Diagram in the Laguerre Geometry and Its Applications. *SIAM Journal on Computing* 1985, 14 (1), 93-105.

[25] CHIARAVALLE, A. G.; COTABARREN, I. M.; PIÑA, J. DEM breakage calibration for single particle fracture of maize kernels under a particle replacement approach. *Chemical Engineering Research and Design* 2023. DOI: 10.1016/j.cherd.2023.05.015.

[26] LVOV, V.; CHITALOV, L. Semi-Autogenous Wet Grinding Modeling With CFD-DEM. *Minerals* 2021. DOI: 10.3390/min11050485.

[27] OPALEV, A. S.; PALIVODA, A. A. Modeling of the liquid-solid particle system in the coupling solution of the task in rocky dem and ansys fluent. *MINING INFORMATIONAL AND ANALYTICAL BULLETIN* 2023. DOI: 10.25018/0236_1493_2022_121_0_78.

[28] BENGTSSON, M.; EVERTSSON, C. M. Modelling of output and power consumption in vertical shaft impact crushers. *International Journal of Mineral Processing* 2008, 88 (1-2), 18-23.

[29] TAVARES, L. M. F. P. P. A. J. C. Adapting a breakage model to discrete elements using polyhedral particles. *Powder Technology: An International Journal on the Science and Technology of Wet and Dry Particulate Systems* 2020, 362.

[30] ANDRÉ, F. P.; TAVARES, L. M. Simulating a laboratory-scale cone crusher in DEM using polyhedral particles. *Powder Technology* 2020. DOI: 10.1016/j.powtec.2020.06.016.

[31] FLÁVIO, P. A.; LUÍS MARCELO, T. Simulating a laboratory-scale cone crusher in DEM using polyhedral particles. *Powder Technology* 2020.

[32] UNLAND, G.; AL-KHASAWNEH, Y. The influence of particle shape on parameters of impact crushing. *Minerals Engineering* 2009, 22 (3), 220-228.

[33] FANG, H. Y.; YANG, J. H.; CHEN, Q. Particle size distribution and energy consumption during impact crushing of single granite particles. *Journal of the Southern African Institute of Mining & Metallurgy* 2018, 118 (5), 555-561.

[34] BUENO, M. P.; KOJOVIC, T.; POWELL, M. S.; SHI, F. Multi-component AG/SAG mill model. *Minerals Engineering* 2013, 44, 12-21.

[35] RODRIGO; M; DE; CARVALHO; AND; LUÍS; MARCELO; Tavares. Predicting the effect of operating and design variables on breakage rates using the mechanistic ball mill model. *Minerals Engineering* 2013.